

Original Article

ANTITUMOR EFFECTS AND CHARACTERIZATION OF BIOSYNTHEZED IRON OXIDE NANOPARTICLES USING SEAWEEDS OF GULF OF MANNAR

SANGEETHA N*, A. K. KUMARAGURU

¹Department of Marine and Coastal Studies, Madurai Kamaraj University, Madurai-21, ²Vice chancellor Manonmaniam sundaranar University Thirunelveli Tamil Nadu, India.
Email: sangeethaplasmodium@gmail.com

Received: 31 Oct 2014 Revised and Accepted: 22 Nov 2014

ABSTRACT

Objective: Three different seaweeds were used for biosynthesis of iron oxide nanoparticles. The screening of seaweeds, and suitable conditions for iron oxide nanoparticle synthesis were analyzed using different optimizing parameters such as concentration of seaweed extract, reaction temperature, and pH. It was found that only one seaweed, *Sargassum myriocystum* was able to synthesized iron oxide nanoparticles.

Methods: Biosynthesized iron oxide particles were characterized and confirmed through the techniques such as X-ray diffraction, Atomic force microscopy, Scanning electron microscope, Transmission electron microscopy and Fourier transform spectroscopy.

Results: Transmission electron microscopy showed image size of iron oxide nanoparticles as 6 - 12 nm. This biosynthesized *S. myriocystum* leaf extract biomolecules act as precipitating and capping agent. Formulation of biosynthesized iron oxide nanoparticle with cancer drug flutamide showed *in-vitro* drug release of 91% which was confirmed with standard flutamide curve. Drug carrier effect in tumors cell through *in vivo* assay was done to analyze life span of mice, liver enzymes and hematological parameters. Overall results of *In-vivo* assay indicated that biosynthesized iron oxide nanoparticles act as good tumor targeted drug carrier with antitumor effect.

Conclusion: As evident from the present study, *S. myriocystum* leaf extract can be used for synthesis iron oxide nanoparticles of 2.8 nm. Biosynthesized iron oxide being smaller and narrow in size which has been used for various types of cancer treatment they were selected further for *in-vitro* and *in-vivo* analysis.

Keywords: Antitumor effect, Cancer, Flutamide, Gulf of Mannar, Iron oxide nanoparticles, Seaweeds.

INTRODUCTION

Nanoparticles have one or more dimensions of the order of 100 nm or less they have attracted great attention due to their unusual and fascinating properties. Their applications are advantageous over their bulk counterparts[1]. Physical methods such as gas phase deposition and electron beam lithography incorporate elaborate procedures that suffer from the inability to control the size of particles[2] in the nanometer size range. Chemical procedures in the synthesis of these NPs involve toxic solvents, which could potentially generate unsafe and hazardous byproducts causing high energy consumption also[3]. Magnetic iron oxide NPs with long blood retention time, biodegradability and low toxicity have become as one of the primary nanomaterials for biomedical applications *in vitro* and *in vivo*. Due to their low toxicity, magnetic iron oxides, such as magnetite (Fe₃O₄) and maghemite (γ -Fe₂O₃), have been used as potential components in biomaterials [4].

Increasing number of medical applications, including drug targeting, bioseparation processes and cancer chemotherapy have been found for iron oxide nanoparticles. The biologically diverse marine environment has a great promise for nanoscience and nanotechnology. A potent non-steroidal anti-androgen, Flutamide (2-methyl-N-[4-nitro-3-(trifluoromethyl) phenyl] propanamide), was used in the palliative treatment of prostatic carcinoma[5].

Treatment with flutamide may cause a variety of side-effects such as diarrhea, tiredness, impotence, breast fullness and liver malfunction [6]. It is essential to develop cost-effective and less tedious procedures for preparation of sustained release formulations in the industrial scale. For that reason we successfully formulated with biosynthesized iron oxide nanoparticles. However, till date only few reports are available on the synthesis of NPs using seaweeds. Hence the present investigation was aimed to study the biosynthesis of iron oxide nanoparticles from freshly collected seaweeds. The biosynthesis process was optimized under various physico-chemical parameters such as, reaction temperature, reaction pH, and time. Further, the characterization of synthesized nanoparticles (NPs) was carried out by

various techniques viz., Atomic Absorption spectrometry measurements, Scanning electron Microscopy and Energy dispersive X-ray analysis, Transmission electron Microscopy and Fourier Transform Infrared Spectroscopy. The biosynthesized iron oxide nanoparticles were also investigated for drug delivery studies.

MATERIALS AND METHODS

Seaweeds Identification and preparation of seaweed extracts

Seaweeds were collected from Kilakarai coast of the Gulf of Mannar region, India and identified using keys available [7]. Samples were rinsed with sea water to remove debris and epiphytes. About 10 g of seaweed was finely cut into small pieces and weighed before transferring into a 500-ml beaker containing 100 ml distilled water, mixed well and then boiled for 25 min. The extract obtained was filtered through Whatman No.1 filter paper and the filtrate was collected in a 250-ml Erlenmeyer flask and stored in a refrigerator at 4°C for further use.

Biosynthesis of iron nanoparticles

Iron oxide nanoparticles were prepared by adding ferric chloride (2%), ferrous sulphate (1%) solution, to the *Sargassum myriocystum* extract (5 ml) and precipitated with 2 ml sodium hydroxide (0.1M). The pH of the solution was controlled by means of a buffer solution, fixing the values at 5, 7, and 10 while stirring vigorously. An orange precipitate immediately formed. The prepared emulsion was placed on a magnetic stirrer and stirred for 1 hour at room temperature. This procedure was applied to three different seaweed filtrates.

Optimization of physico-chemical parameters for metal nanoparticle biosynthesis

Metal nanoparticles syntheses were carried out from three different seaweeds. Only ferric chloride (2%) and ferrous sulphate (1%) solutions were used in all the reactions. Temperature was maintained at 50, 60, 70, 80,90 and 100° C using a water bath and pH was maintained at 5, 6, 7, 8, 9 and 10, which was adjusted using

0.1 M HCl or 0.1 M NaOH; duration of reaction time was maintained from 1hr to 72 hrs.

Centrifugation and Lyophilization metal nanoparticles

To remove the non-metal components for maximum recovery of metal nanoparticles from the synthesized solution, an optimal centrifugation process was obtained based on tests of two centrifugation forces 12,000 and 15000 rpm for 30 min. The process of centrifugation and redispersion in sterile deionized water was repeated thrice to obtain better separation of entities from the metal nanoparticles. The purified solution of metal nanoparticles were then freeze dried using a lyophilizer (Micro Modulyo 230 freeze dryer, Thermo Electron Corporation, India). Then the dry powder was mixed with 10 ml deionised water and kept on a sonicator to prevent aggregation of ions.

Characterization of metal nanoparticles

The synthesized nanoparticles were characterized by various techniques viz., Dynamic light Scattering (DLS) (Size Distribution Report by Intensity - Malvern Instruments Ltd, Zetasizer Ver. 6.20 Serial Number: MAL1052893), Atomic Force Microscopy (AFM) measurements images were collected using a Digital Instruments Nanoscope microscope at 27 °C. Etched Si nitrate nanoprobe tips (APE Research- model no: A100SGS) were used with Scanning Electron microscopy (SEM) (SEM-EDX JEOL Model-L6390). The size and elemental status of metal nanoparticles were confirmed by SEM EDX. Transmission electron microscopy (TEM) operated under vacuum in the order of 10^{-7} torr, equipped with an electron gun capable of accelerating electrons through a potential difference in the range of 60 to 300kV (Jeol JEM-2100F transmission electron microscope was used).

A thin sample fixed on the grid was illuminated by an electron beam to perform analysis in the TEM. The biosynthesized nanoparticles solution was drop-coated onto glass substrate and powder X-ray diffraction measurements were carried out in an X-ray diffractometer (Shimadzu- model XRD 6000). Dried powder of biosynthesized nanoparticles were analyzed using FTIR (Model 8400 s SHIMADZU). A disk of KBr was prepared with a mixture of finely dried sample (1: 3 ratio) and then examined under IR-Spectrometer. Infrared spectra were recorded in the region of 500 to 4000 cm^{-1} . Thus important information for the understanding of different physicochemical features were gathered.

Nanoparticle as a drug delivery vehicle for cancer therapy

Formulation of Iron Nanoparticles with cancer drug

0.5 mL Calcium chloride (18 mM) was added to 4.5 mL of sodium alginate solution (0.06%) containing the drug flutamide (10 mg). 2 ml of iota carrageenan solution (0.05%) was added followed by stirring for 30 min and then iron nanoparticles solution 2 ml (0.5mg) was added and kept at room temperature overnight. Drug-free nanoparticles were also prepared in the same manner.

The prepared emulsion was placed on a magnetic stirrer and stirred for 12 h at room temperature. Drug-loaded nanoparticles were recovered by centrifugation at 19000 rpm for 35 min and washing three times with distilled water [8].

In vitro drug release

For the drug release efficiency tests, the nanoparticles suspension was analyzed in 4 different concentration samples. *In vitro* release study was performed on suspension of nanoparticles within 24 h of preparation. The prepared flutamide solution with iron nanoparticles was sonicated for 1 min. Sonicated samples were transferred to an open ended cylinder sealed by cellophane membrane (soaked glycerol water 2:1 before 24 h) and subjected to dialysis by immersing the dialysis tube to receptor compartment containing 200 ml of phosphate buffer solution (pH 7.4.) The medium in the receptor was agitated continuously using a magnetic stirrer. At the time intervals of every 1h up to 24h, 1 ml of phosphate buffer solution was taken and replaced with the same amount of fresh medium. Thereafter the amount of drug in the water phase

was detected by a UV-Vis spectrophotometer at 307 nm. The test was repeated thrice [9].

In vivo study of iron oxide nanoparticles

Selection grouping and acclimatization of laboratory animals

Male Swiss albino mice (20-25 gm) were procured from central animal house, and used throughout the study. They were housed in micro nylon boxes in a controlled environment (temperature $25 \pm 2^\circ\text{C}$) and 12 h dark /light cycle with standard laboratory diet and water. The study was conducted at K. M College of Pharmacy Madurai, Tamil Nadu, India. The study was conducted after obtaining institutional animal ethical committee clearance (N. Sangeetha /F8028/IAEC/KMCP/38/2012). As per the standard practice, the mice were segregated based on their gender and quarantined for 15 days before the commencement of the experiment. They were fed with healthy diet and maintained in hygienic environment in the animal house. Dalton's Lymphoma Ascites (DLA), and Ehrlich Ascites Carcinoma (EAC) methods were used in experimental studies of anticancer activity [10].

Treatment protocol and treatment

Animals were divided into four groups consisting of six animals in each group: group 1, served as normal control; group 2, DLA cells served as tumor control; group 3, served as Treatment control, and treated with injection of flutamide at 10 mg/kg body weight [11], group 4 served as Treatment control group and was administered iron oxide nanoparticles preparation of flutamide in a dose of 10 mg/kg intra peritoneally. All animals in the four groups were injected with DLA cells (1×10^6 cells per mouse) intra peritoneally to develop carcinoma and the remaining one group was the normal control group. In this study, drug treatment was given after 48 hrs of inoculation of tumour cell, once daily for 14 days. After the last dose, all mice from each group were sacrificed. Blood was withdrawn from each mouse by retro orbital puncture method and the clinical parameters were checked [12].

Evaluation of clinical parameters and hematological parameters

The fluid (0.1 ml) from the peritoneal cavity of each mouse was withdrawn by sterile syringe and diluted with 0.8 ml of ice cold Normal saline or sterile Phosphate Buffer Solution and 0.1 ml of trypan blue (0.1 mg/ml) and total number of the living cells was counted using a haemocytometer [13].

$$\text{Cell count} = \text{No of cells Dilution} / \text{Area} \times \text{Thickness of liquid film}$$

Blood samples were collected from each mouse by retro orbital plexus method. Whole blood was collected in ethylene-diamine-tetra-acetic acid coated vials for examination of potential hematologic toxicity. Hematologic analysis included determination of white blood cell, red blood cell, hemoglobin, platelet levels and packed cell volume.

Serum enzyme and lipid profile analysis

Liver enzyme and lipid profile analysis were done using an automated hematologic analyzer (COBAS MIRA PLUS-S -Roche Switzerland) for Aspartate amino Transferase (AST), Alanine amino Transferase (ALT), Alkaline Phosphatase (ALP), Total Cholesterol (TC) and Triglyceride (TG). Abnormal blood lipid profile has been associated with cancer. In Hodgkin lymphoma, high cholesterol level and low triglyceride level have been reported and investigated in this parameter study [13].

Derived parameters

All the mice were weighed, from the beginning to the 15th day of the study. Average increase in body weight on the 15th day was determined. % ILS was calculated by the following formula. All biochemical investigations were done using OBAS MIRA PLUS-S Auto analyzer from Roche Switzerland. Hi-Tech instruments viz., MAX MAT were used for auto analysis [14].

$$\frac{\text{Life span of treated group}}{\text{Life span of control group}} - 1 \times 100$$

RESULTS AND DISCUSSION

Screening of seaweed and optimization of iron oxide nanoparticles

Preliminary biosynthesis of nanoparticles was performed with three different Seaweeds for the optimum production of metal nanoparticles. The biosynthesis reaction started within few minutes when 5 ml seaweed extract was subjected to 2% ferric chloride, 1% of ferrous sulphate solution and the formation of metal nanoparticles.



Fig. 1: Morphology of green Seaweed *Caulerpa scapelliformis* (Lamouroux 1809)



Fig. 2: Morphology of Red Seaweed *Laurencia papillosa* (Greville 1830)



Fig. 3: Morphology of Brown Seaweed *Sargassum myriocystum* (Agardh, 1848)

The preliminary screening showed that leaf extracts of seaweed *Sargassum myriocystum* exhibited synthesis of iron oxide nanoparticles. Iron nanoparticles were prepared by adding a seaweed extract to an aqueous mixture of Fe^{2+} and Fe^{3+} chloride as 1:2 molar ratio. The precipitated magnetite is brown in color. Shen

et al. (1999) observed that the product showed a brownish color, an indication of the presence of Fe_2O_3 . According to the thermodynamics of this reaction, a complete precipitation of Fe_3O_4 should be expected between pH 9, while maintaining a molar ratio of $\text{Fe}^{3+}:\text{Fe}^{2+}$ is 2:1 under a non-oxidizing oxygen free environment [15].

Another important factor influencing the synthesis is iron concentration. Moreover, only small quantities of $\text{Fe}^{3+}:\text{Fe}^{2+}$ in 2:1 ratio is necessitated by biosynthesis procedure. Generally the concentration optimum values are between 39 and 78 mM. Smaller and more uniform particles were prepared by biosynthesis method of magnetite at low temperature 90°C at pH 9, while higher reaction temperatures ($>80^\circ\text{C}$) favor the formation of Fe_3O_4 [16-17]. At the same time the sample temperature was 50°C to 80°C and above 100°C there was no characteristic peak observed.

pH should be noticed that the tendency to produce smaller and more controlled particles is improved by increasing the value of the pH 11 (9 and 11 are better than 3 and 5)[18]. The pH value of the reaction mixture has to be adjusted in both the synthesis and purification steps. As a result, there was the production of significant quantities of narrowly dispersed, nanometer sized magnetic particles through biosynthesis method. But in the case of chemical precipitation method, aggregation remains a significant challenge in this method. So the critical difficulty is that these particles form aggregates and grow to minimize the overall surface free energy, so that free precipitation is not a viable technique [19-20].

Characterization of Iron nanoparticles

X-ray diffraction analysis

The biosynthesis method has been used to generate novel materials with unusual properties. A typical XRD pattern of iron oxide nanoparticles was seen. A number of Bragg reflections with 2θ values of 32.2° , 45.5° , 56° and 66.6° corresponding to (111) (113) and other low intensity planes, were observed Fig.4. The XRD pattern thus clearly illustrates the iron oxide nanoparticle synthesized by the *Sargassum myriocystum*. All peaks of the diffractogram are in agreement with the theoretical data of hematite (JCPDS card no. 33-0664).

The crystallite size was calculated using Debye-Scherrer formula and the size was found to be 28 nm. Average size of the iron oxide nanoparticles was determined from the width of the reflection according to the Debye-Scherrer equation. By considering the FWHM of the dominant (113) diffraction peak of iron oxide nanoparticles, the crystalline size of the iron oxide was calculated as 28 nm. The crystalline iron oxide peaks (113) resulted due to bio-organic compounds/proteins in the nanoparticle during the synthesis [21-24].

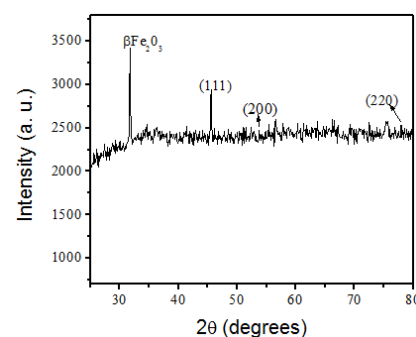


Fig. 4: X-ray diffraction pattern at $2\theta: 20^\circ - 80^\circ$ for Iron oxide nanoparticles

AFM Analysis of synthesized Iron oxide nanoparticles

The synthesized iron oxide nanoparticles are almost spherical in shape. Similar result was observed by SEM analysis. The average height of the particles on the substrates and uniform height distribution was around 15 nm (Fig.5 b).

The AFM images (fig. 5a and 5 b) show three dimensional view of sample surface over a $2 \times 2 \mu\text{m}$ scan and uniform height distribution around 15 nm. The size of monodispersed single iron oxide nanoparticle was 8 nm. The tendency of iron oxide nanoparticle to form the aggregate indicated the existence of an attractive interaction among the nanoparticles.

The particle size 11- 18 nm distribution was calculated using gwyddion 2.9 analysis software. The broad surface area of the nanoparticles and the magnetic forces between them could cause a considerable agglomeration between the fabricated Fe_3O_4 magnetite nanoparticles [25].

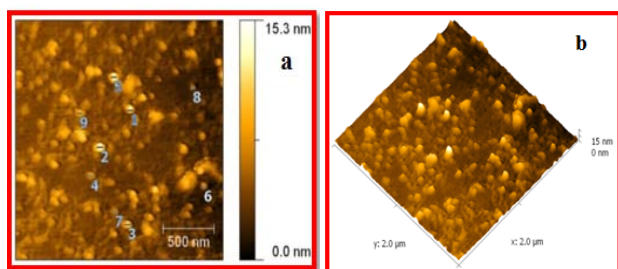


Fig. 5: AFM results of iron nanoparticles 2D and 3D images (a) AFM 2D image showing iron oxide nanoparticles (b) 3D image of biosynthesized iron oxide nanoparticles

SEM and EDX analysis

From the SEM image the size of the iron oxide NPs was found to be 44 - 81 nm. The shape of most of the synthesized nanoparticles appeared spherical and in few cases, they formed small aggregates. Fig.6 shows that Fe and O are present in the sample. No presence of secondary peak indicated that the nanoparticles were spherical in shape, which is same in AFM analysis. EDX spectroscopy confirmed the significant presence of iron oxide.

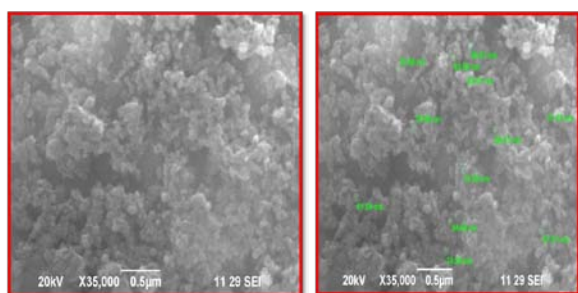


Fig. 6: SEM images of Iron oxide nanoparticles

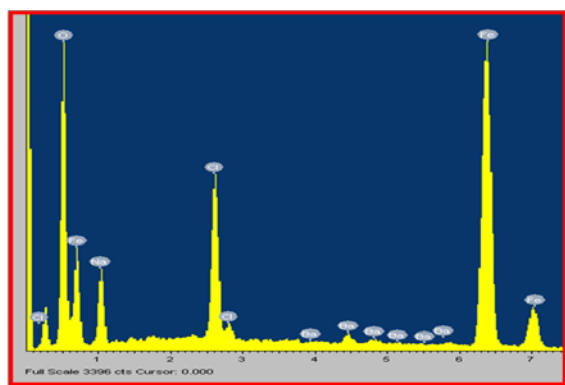


Fig. 7: EDX spectrum of Iron oxide nanoparticles

Table 1: Elemental composition of Iron oxide nanoparticles

Element	Weight %	Atom %
Fe	56.02	60.48
O	19.26	38.85
Na	0.31	1.30
Total		100

TEM analysis

TEM image shows that not all particles are ideally round and that there is a fluctuation in size. Most of the particles show an almost spherical shape and size of the particles are up to 6 nm in diameter while others are in between 6 and 12 nm. This could be attributed to the fact that the magnetic nanoparticles were so small that they may be considered to have a single magnetic domain. The smaller nanoparticles that form the bigger aggregates were about 6 - 12 nm in diameter [26].

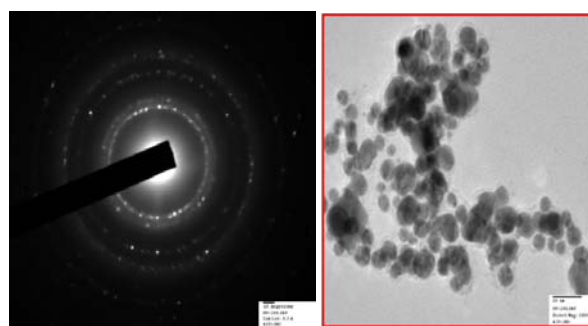


Fig. 8: TEM result of iron oxide nanoparticles

Analysis of chemical nature before and after synthesis, FTIR Analysis

FTIR measurements were carried out to identify the possible biomolecules responsible for capping and efficient stabilization of iron nanoparticles synthesized using *S. myriocystum* extract. The bands of biosynthesized iron oxide nanoparticles from *S. myriocystum* were noticed at 3422, 1621, 1409 and 1039 cm^{-1} in the FTIR spectrum. Whereas, bands of *S. myriocystum* extract were noticed at 3465, 2388, 1652 1070 and 584 cm^{-1} .

The stretching vibrations of hydroxyl groups (OH) usually form a broad band region at 3465-3422 cm^{-1} . After Fe_3O_4 nanoparticles are functionalized with biomolecules, the stretching vibration of hydroxyl groups disappears, while a C-H stretching vibrating band at 2921 and 2911 cm^{-1} arises and a carboxylic group transmittance at 1621 and 1409 cm^{-1}

The IR spectra of iron oxide exhibit strong bands in the low frequency region (1000 - 400 cm^{-1}) due to the iron oxide skeleton and the spectrum is highly consistent with magnetite (Fe_3O_4) spectrum bands at 440 and 1031 cm^{-1} and in other regions, the spectra of iron oxide have weak bands. Fig. 9 clearly showed the O-H stretching vibrations at 3430 cm^{-1} and C-H stretching vibrations at 2925 cm^{-1} which were sharper and broader than the iron oxide NPs.

The band at 1650 cm^{-1} can be characteristic of the antisymmetric stretching of C = C alkene groups which is in accordance with the high uronic content [27-29]. It could be confirmed that, water-soluble alginate in the extract played complicated roles in the bioreduction of the precursors and shape evolution of the nanoparticles. Fucoic acid might be responsible for material reduction in the *S. myriocystum* leaf extract. This biosynthesis with *S. myriocystum* leaf extract for biomolecules acts as a precipitating and capping agent [30]. All the above observations found in the IR spectra confirmed the presence of iron oxide nanoparticles.

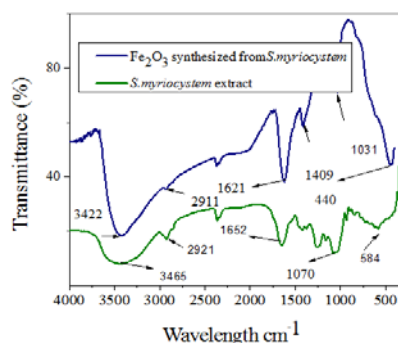


Fig. 9: FTIR-Transmittance spectra of *S. myriocystum* before and after reduction of iron oxide nanoparticles

Nanoparticle as drug delivery vehicle for cancer therapy

In vitro iron oxide nanoparticles drug release

Based on drug content, *in vitro* release of the formulations showed good uniformity in drug content and the percentage of drug content was 91%. The cumulative percentage of drug release from flutamide iron nanoparticles after 24 hours the maximum amount of drug was released and the AFM size was 16 nm. The entrapment and release rates of the flutamide drugs from the drug flutamide with iron oxide nanoparticles increased with increasing cross-linking agent concentration[31]. The amount of bound drug and the type of interaction of drug and nanoparticles depend on the chemical structure of the drug as well as the polymer and the conditions of drug loading.

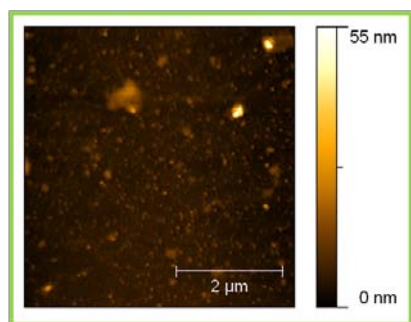


Fig. 10: 2D image of formulated iron oxide nanoparticles with flutamide

Table 2: Effect of Iron oxide nanoparticles formulation on the Life Span, Body Weight and Cancer Cell Count of Tumor Induced Mice

Treatment	Number of animals	% ILS Life span	Body weight in grams	Cancer cell count ml X 106
G1	6	>>30 days	2.26±0.45	-
G2	6	50%	7.66±1.05a**	2.65±0.40a**
G3	6	80%	5.35±0.86b*	1.90±0.30a*
G4	6	92%	3.65±0.58b**	1.28±0.11b**

G1 – Normal Control, G2 – Cancer Control, G3 – Treatment control (flutamide 10mg/kg), G4 – Treatment control (Nanoparticle of flutamide 10mg/kg).

All values are expressed as mean ± SEM (n=6).

a** – Values are significantly different from control (G1) at P < 0.001

b* – Values are significantly different from cancer control (G2) at P < 0.01

b** – Values are significantly different from cancer control (G2) at P < 0.001

***In vivo* study of iron oxide nanoparticles:** In the present study, the particle size of iron oxide nanoparticles was 6 - 12 nm. The present investigation was carried out in treatment with flutamide and flutamide iron oxide nanoparticles at the dose of

Hematologic analysis

In the Dalton's Lymphoma ascites (DLA) tumor control group, the average life span of mice was 50% whereas, treatment with flutamide at a dose of 10 mg/kg body weight increased the life span to 80%. However, the average life span of flutamide iron nanoparticles treatment was 92%.

The antitumor nature of the flutamide iron nanoparticle was evident by the significant reduction in percent increase in body weight of animals treated with the flutamide iron nanoparticle at the dose of 10mg mg/kg body weight when compared to DLA tumor bearing mice. It was also supported by the significant reduction in viable tumor cell count in both treatments compared to the DLA tumor control (Table 2).

Comparative analysis of various hematologic parameters in the flutamide and flutamide iron nanoparticles treated mice and control animals is given in table 3. RBC, Hb and Platelets decreased whereas, WBC count significantly increased in the DLA control group compared to the normal control group. Treatment with flutamide, and flutamide iron nanoparticles at the dose of 10mg/kg significantly increased the content of Hb, RBC, Platelets and significantly decreased the WBC count to about normal level.

The inoculation of DLA cells caused significant increase in the level of total Cholesterol, Aspartate amino Transferase (AST), Alanine amino Transferase (ALT) and Alkaline Phosphatase (ALP) in the tumor control animals (G₂), compared to the normal group. Treatment with the compound at the dose of 10mg /kg body weight reversed these changes towards normal level (Table 4).

Histopathology analysis

The histological sections under microscope (Fig. 11a) showed structure of normal control liver (G₁) of male swiss albino mice with sheets of hepatocytes separated by sinusoids, central vein and portal tract appearing normal. On the other hand, sections (Fig. 11b) of tumor control liver (G₂) of male swiss albino mice, presented mild hepatic congestion at sinusoids and the portal vessel, pericentre globular micro-steatosis, no kuffe cell proliferation, mild hepatocyte diffuse necrosis and mononuclear infiltrate.

Flutamide treated tumor liver (G₃) of male swiss albino mice showed (Fig. 12 a) hepatic congestion at sinusoids and the portal vessel, pericentre globular micro-steatosis, kuffe cell proliferation, hepatocyte diffuse necrosis and mononuclear infiltrate. Whereas, sections (fig. 12 b) of flutamide formulated with biosynthesized iron oxide nanoparticles treated tumor liver(G₄) of male swiss albino mice showed moderate hepatic congestion at sinusoids and the portal vessel, pericentre globular micro-steatosis, less kuffe cell proliferation, mild hepatocyte diffuse necrosis and mononuclear infiltrate.

10 mg/kg body weight that inhibited the tumor volume, viable tumor cell count and increased the life span of the tumor bearing mice. The reliable criteria for judging the value of any anticancer drug are the prolongation of the lifespan of animals [32].

Table 3: Effect of Iron oxide nanoparticles formulation on hematological parameters

Treatment	Total WBC Cells /mlx10 ³	RBC Count Millon/cumm	Hb gm/dl	PCV in %	Platelets Lakhs/cumm
G1	9.85 ±1.45	4.55±0.96	12.52 ±1.22	14.55±2.36	3.20±0.92
G2	14.82 ±2.7a**	2.45±0.6a**	7.22 ±0.9a**	32.60±4.6a**	1.60±0.4a**
G3	12.22 ±2.1b*	3.12±0.6b*	9.32±0.9b*	27.15±3.7b*	1.88±0.6b*
G4	11.26±1.7b**	4.06±0.8b**	11.60 ±1.2b**	18.22±2.5b**	2.72±0.8b**

G1 – Normal Control, G2 – Cancer Control, G3 – Treatment control (flutamide 10mg/kg), G4 – Treatment control (Nanoparticle of flutamide 10mg/kg)

All values are expressed as mean ± SEM (n=6).

a** – Values are significantly different from control (G1) P < 0.001

b* – Values are significantly different from cancer control (G2) P < 0.01

b** – Values are significantly different from cancer control (G2) P < 0.001

The major criteria to be taken into consideration for any potential anti tumour drug are its efficacy in prolongation of lifespan and decrease of tumor volume and viable tumor cell count [33].

Based on drug content, particle size morphology and *in vitro* release, optimum formulation was selected. Thus nanoparticles of flutamide with iron oxide nanoparticles was found to be spherical, discrete

and free flowing and able to sustain the drug release effectively. In DLA tumor bearing mice, a regular rapid increase in ascitic tumor volume was observed as suggested [34-35]. According to Prasad and Giri ascitic fluid is the direct nutritional source for tumor cells and a rapid increase in ascitic fluid with tumor growth would be a means to meet the nutritional requirement of tumor cells.

Table 4: Effect of Iron oxide nanoparticles formulation on serum enzymes and lipid proteins

Treatment	Cholesterol (mg/dl)	TGL (mg /dl)	AST (U/L)	ALT (U/L)	ALP (U/L)
G1	99.19±3.75	122.95±2.42	37.36 ±1.18	36.35 ±1.3	126.2 ±2.2
G2	142.22±4.7a**	209.22±4.7a**	86.5±2.8a**	62.25±2.6a**	242.2±4.3a**
G3	130.40±3.6b*	190.28±3.4b*	70.26 ±2.2b*	56.32±1.8b*	195.3±2.4b*
G4	112.24±3.1b**	160.35±3.1b**	54.30 ±1.6b**	42.35±1.3b**	162.3±2.4b**

G1 – Normal Control, G2 – Cancer Control, G3 – Treatment control (flutamide 10mg/kg), G4 – Treatment control (Nanoparticle of flutamide 10mg/kg).

All values are expressed as mean ± SEM (n=6).

a** – Values are significantly different from control (G1) P < 0.001

b* – Values are significantly different from cancer control (G2) P < 0.01

b** – Values are significantly different from cancer control (G2) P < 0.001

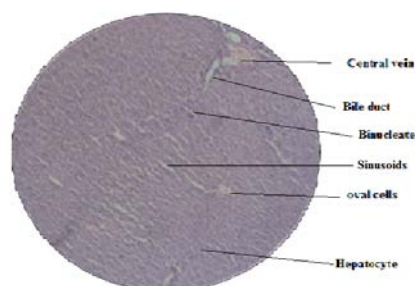


Fig. 10: a. Tumor Control section shows structure of liver of mice

Usually, in cancer chemotherapy, the major problems that are being encountered are myelo suppression and anemia[11]. The anemia encountered in tumor bearing mice is mainly due to reduction in RBC or Hb and this may occur either due to iron deficiency or due to hemolytic or myelopathic conditions [36]. Treatment with flutamide and flutamide iron nanoparticles at the dose of 10 mg/kg body weight brought back the (Hb) content; RBC and WBC count more or less to normal levels significantly.

This clearly indicates that flutamide iron oxide nanoparticles at the dose of 10 mg/kg body weight possess protective action on the haemopoietic system. These data highlight the nontoxic effect of the iron oxide nanoparticles, which did not induce any alteration in hematologic parameters in treated mice when compared with controls and, at the same time, led to effective control of white blood cells that possess the immunologic constituents of ascitic fluid. Data obtained from these studies could help us to further optimize the

formulation, if necessary, and to enhance the efficiency of our MNPs for drug delivery applications.

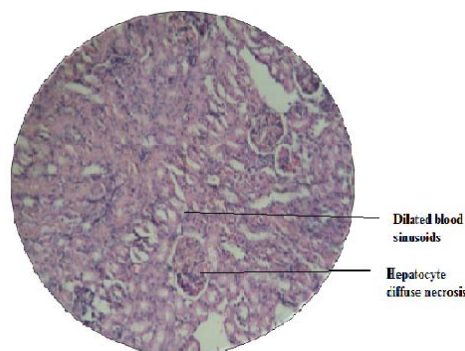


Fig. 10: b. Normal control section shows structure of liver of the mice

There are a number of possible mechanisms for the appearance of abnormal activities of enzymes in serum. Enzymes in serum have been studied for many years as possible early indicators of neoplasia, since it aids in following the progression and regression of disease. It was reported that the presence of tumour in the human body or in the experimental animals is known to affect many functions of the liver, even when the site of the tumor does not interfere directly with organ functions [37].

Normally, the liver damage and the loss of functional integrity of cell membrane are the significant changes in the tumor inoculated animal and is indicated by elevated levels of total cholesterol, TG, AST, ALT and ALP in the serum, whereas, the treatment with the

flutamide iron oxide nanoparticles significantly made reversal of these changes towards normal and it did not cause any damage to the liver functions. Thus these results support the potent vehicle for antitumor and hepato protective nature of the flutamide iron oxide nanoparticles compared to flutamide.

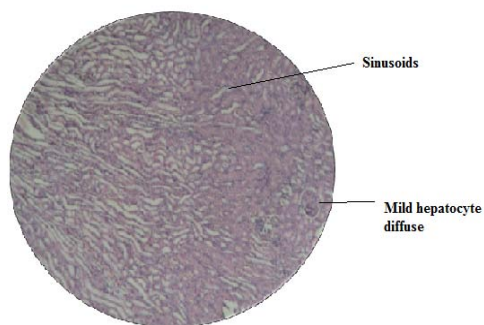


Fig. 11: a. Treatment control flutamide section shows structure of liver of mice

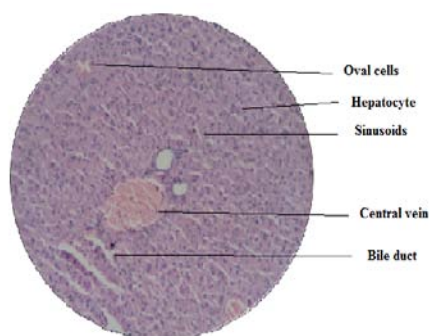


Fig. 11: b. Treatment control flutamide with iron Nanoparticles section shows structure of liver of mice

In the present study, the biochemical examination of DLA inoculated animals showed marked changes indicating the toxic effect of the tumor. The normalization of these effects observed in the serum treated with flutamide iron oxide nanoparticles at the dose of 10 mg/kg body weight possesses significant antitumor and hepatoprotective effect of the extracts. Our serum iron data do not discriminate between bound and free forms of iron, but it appears that most of the iron in the body is in the bound form because of its slow clearance kinetics[38]. This may be due to its inhibitory activities in several signaling cascades responsible for the development and pathogenesis of the disease which are not yet understood. Taken together, the data suggest that the flutamide iron oxide nanoparticles can induce cytotoxic effects on DLA cells, act as vehicle for tumor treatment and thereby effectively controlling disease progression without toxicity to normal cells. Histological analyses of liver samples showed no apparent abnormal changes. Thus the flutamide iron oxide nanoparticles serve as a drug delivery vehicle for cancer therapy by decreasing progressive development of tumor cells.

CONCLUSION

As evident from the present study, *S. myriocystum* leaf extract can be used for synthesis iron oxide nanoparticles of 2.8 nm. Biosynthesized iron oxide being smaller and narrow in size which has been used for various types of cancer treatment they were selected further for *in-vitro* and *in-vivo* analysis. *In-vitro* study of iron oxide nanoparticle with cancer drug flutamide studies revealed that the iron oxide nanoparticles act as good drug carrier (drug release 91%). *In vivo* assay concluded that hematology and histopathology analysis studied for the biochemical examination of DLA inoculated mice showed marked changes indicating the toxic

effect on the tumor cells, and it has significant antitumor and hepatoprotective activity. Linear progression in the body weight of tumor bearing mice with advancement of duration was also observed in this study. Such increase in body weight was significantly retarded following the iron oxide treatment. Most antitumor drugs are anti proliferative and will also affect radically dividing normal cells. Treatment with the flutamide with iron oxide nanoparticles also increased the life span of the tumor bearing mice. It may be concluded flutamide nanoparticles at the dose of 10 mg/kg body weight by decreasing the nutritional fluid volume and arresting the tumor growth, increases the life span of DLA bearing mice. Thus flutamide nanoparticles at the dose of 10 mg/kg body weight have antitumor activity against DLA bearing mice. These results revealed that, these biosynthesized iron oxide nanoparticles appear to be a promising vehicle for tumour targeted drug delivery.

ABBREVIATION

2D, Two dimension; 3D, Three dimension; AFM, Atomic force microscope; ALP, Alkaline Phosphatase; ALT, Alanine amino Transferase; AST, Aspartate amino Transferase, cm, Centimeter; DLS, Dynamic light scattering; DLA, Dalton's Lymphoma Ascites; EDX, Energy dispersive x-ray analysis; eV, Electron volt; Fig., Figure; Fe₂O₃, Iron oxide; FTIR, Fourier transform infrared spectroscopy; FWHM, Full width of half maximum; g, Gram; HCL, Hydrochloric acid; IR, Infrared; M, Molar; min, Minute; ml, Milliliter; mM, Milli molar; NaOH, Sodium hydroxide; nm, Nanometer; NPs, Nanoparticles; PDI, Polydispersity index; RBC, Red blood cells; Rpm, Revolutions per minute; SEM, Scanning electron microscope; SPR, Surface plasmon resonance; TEM, Transmission electron microscopy; Vis, Visible; WBC, White blood cells; XRD, X-ray diffraction.

COMPETING INTEREST

The authors confirm that this article content has no competing interest.

ACKNOWLEDGEMENT

I take this opportunity to sincerely acknowledge the University Grants Commission, New Delhi, for providing financial assistance in the form of a BSR JRF and senior Research Fellowship to perform my work comfortably. It's my fortune to gratefully acknowledge the support of special individual, Dr. R. Gobal former professor & Head in-charge, Research Dept of zoology Yadava College Madurai, Tamilnadu India.

REFERENCES

1. Kato H. *In vitro* assays: tracking nanoparticles inside cells. Nat Nanotechnol 2011;6(3):139-40.
2. Rishton A, Lu Y, Altman RA, Marley AC, Bian Hahnes C, Viswanathan R, *et al.* Magnetic tunnel junctions fabricated at tenth-micron dimensions by electron beam lithography. Microelectron Eng 1997;35:249-52.
3. Osaka T, Matsunaga T, Nakanishi T, Arkaki A, Niwa D, Iida H. Synthesis of magnetic nanoparticles and their application to bioassays. Anal Bioanal Chem 2006;384:593-600.
4. Yang Hung-Wei, Hua Mu-Yi, Liu Hao-Li, Huang Chiung-Yin, Wei Kuo-Chen. Potential of magnetic nanoparticles for targeted drug delivery. Nanotechnol Sci Appl 2012;5:73-86.
5. Sweetman SC. (ed.) Martindale, Complete Drug Reference. 34th ed. Pharmaceutical Press, London; 2005. p. 556-7.
6. Peng S, Wang C, Xie J, Sun S. Synthesis and stabilization of monodisperse Fe nanoparticles. J Am Chem Soc 2006;128:10676-7.
7. Ganesapandian S, Kumaraguru AK. Seaweeds resource in the intertidal and subtidal regions of pudhumadam Gulf of mannar. Seaweed Res Utilization 2008;30:97-105.
8. Ramachandra Reddy G, Mahaveer S Bhojani, Patrick McConville, Jonathan Moody, Bradford A. Vascular targeted nanoparticles for imaging and treatment of brain tumors. Clin Cancer Res 2006;12:6677-86.
9. Jacqueline MH, Darius JN, Mathew JM, Ronald DB. Blood lipid profile in children's with acute lymphoblastic leukemia. Cancer 1998;83:379-84.

10. Jahan AK, Sulthan S, Rowshanul H, Kumar S, Mosin A. Antineoplastic activity of Bis-Tyrosinediaqu Ni (II) against ehrlich ascites carcinoma. *J Pharm Sci* 2008;7:33-7.
11. Price VE, Greenfield RE. Anemia in cancer. *Adv Cancer Res* 1958;5:199-200.
12. Hogland HC. Hematological complication of cancer chemotherapy. *Semin Oncol* 1982;9:95-102.
13. Viroj wiwanikit. High serum alkaline phosphatase level in hospitalized patient. *BMC Family Practice* 2001;10(1861):1471-2296.
14. Shen L, Laibinis PE, Hatton TA. Bilayer surfactant stabilized magnetic fluids synthesis and interactions at interfaces. *Langmuir* 1999;15:447-53.
15. Gupta AK, Gupta M. Synthesis and surface engineering of iron oxide nanoparticles for biomedical applications. *Biomaterials* 2005;26:3995-4021.
16. Laurent S, Forge D, Port M, Roch A, Robic C, Vander Elst L, *et al.* Magnetic iron oxide nanoparticles: synthesis, stabilization, vectorization, physicochemical characterizations, and biological applications. *Chem Rev* 2008;108(6):2064-110.
17. Ziolo RF, Giannelis EP, Weinstein BA, Ohoro MP, Ganguly BN, Mehrotra V, *et al.* Matrix-mediated synthesis of nanocrystalline ggr-Fe₂O₃: A New Optically Transparent Magnetic Material 1992;10(257):219-23.
18. Igartua M, Saulnier P, Heurtault B, Pech B, Proust JE, Pedraz JL, *et al.* Development and characterization of solid lipid nanoparticles loaded with magnetite. *Int J Pharm* 2002;233:149-57.
19. Nidhin M, Indumathy R, Sreeram KJ, Balachandran Unni Nair. Synthesis of iron oxide nanoparticles of narrow size distribution on polysaccharide templates. *Bull. Mater Sci* 2008;31(1):93-6.
20. Kim DK, Y Zhang, W Voit, KV Rao, J Kehr, B Bjelke, *et al.* Superparamagnetic iron oxide nanoparticles for bio-medical applications. *Scripta Mater* 2001;44:1713-7.
21. Inouye K, Endo R, Otsuka Y, Miyashiro K, Kaneko KT. Ishikawa micelle and reversed microemulsion. *J Phys Chem* 1982;86:1465-9.
22. Canizal G, Ascencio JA, Gardea-Torresday J, Jose-Yacaman M. Multiple twinned gold nanorods grown by bio-reduction techniques. *J Nanoparticle Res* 2001;3:475-81.
23. Rautaray D, Ahmad A, Sastry M. Biosynthesis of CaCO₃ crystals of complex morphology using a fungus and an actinomycete. *J Am Chem Soc* 2003;125(48):146-56.
24. Basavaraja S, Balaji SD, Lagashetty A, Rajasab AH, Venkataraman. A Extracellular biosynthesis of silver nanoparticles using the fungus *Fusarium semitectum*. *Mater Res Bull* 2008;43(5):1164-70.
25. Donini C, Robinson DN, Colombo P, Giordano F, Papas NA. Preparation of poly(methacrylic acid-g-poly(ethylene glycol)) nanospheres from methacrylic monomers for pharmaceutical applications. *Int J Pharm* 2002;245:83-91.
26. Emad al din Haratifar, Hamid Reza Shahverdi, Mojtaba Shakibaie, Kamyar Mollazadeh Moghaddam, Mohsen Amini, Hojatollah Montazeri, *et al.* Semi-Biosynthesis of magnetite-gold composite nanoparticles using an ethanol extract of *eucalyptus camaldulensis* and study of the surface chemistry. *J Nanomater* 2009;1-5:5.
27. Sipos P, Berkesi O, Tombacz E, St Pierre TG, Webb J. Formation of spherical iron (III) oxyhydroxide nanoparticles sterically stabilized by chitosan in aqueous solutions. *J Inorg Biochem* 2003;95:55-63.
28. Hui-li Maa, Xian-rong Qi, Yoshie Maitani suneji Nagai T. Preparation and characterization of superparamagnetic iron oxide nanoparticles stabilized by alginate. *Int J Pharm* 2007;333:177-86.
29. Davis TA, Volesky B, Mucci A. A review of the biochemistry of heavy metal biosorption by brown algae. *Water Res* 2003;37:4311-30.
30. Shenoy D, Little S, Langer R, Amiji M. Poly(ethylene oxide)-modified poly(β -amino ester) nanoparticles as a pH-sensitive system for tumor-targeted delivery of hydrophobic drugs: *in-vitro* evaluations. *Mol Pharm* 2005;2(5):357-66.
31. Clarkson BD, Burchenal JH. Preliminary screening of antineoplastic drugs. *Prog Clin Cancer* 1965;1:625-9.
32. Arora S, Jain J, Rajwade JM, Paknikar KM. Cellular responses induced by silver nanoparticles: *In vitro* studies. *Toxicol Lett* 2008;179:93-100.
33. Adlin, Jino Nesalin, Gowthamarajan K, Somashekhara CN. Formulation and evaluation of nanoparticles containing flutamide. *Inter J Chem Tech Res* 2009;1(4):1331-4.
34. Gupta M, Mazumder U, Sambath Kumar R, Siva Kumar T. Antitumor activity and antioxidant role of *Bauhinia racemosa* against *Ehrlich ascites* carcinoma in Swiss albino mice. *Acta Pharmacol Sin* 2004;25(8):1070-6.
35. Prasad SB, Giri A. Anti tumor effect of cisplatin against murine ascites dalton's lymphoma. *Indian J Exp Biol* 1994;32:155-62.
36. Fenninger LD, Mider GB. Energy and nitrogen metabolism in cancer. *Adv Cancer Res* 1954;2,229-53.
37. De Wys, William D. Pathophysiology of tumour cachexia: current understanding and areas for future research. *Tumour Res* 1982;42:721-5.